PRAMANA — journal of physics | © Indian Academy of Sciences | Vol. 82, No. 4 April 2014 pp. 625–635

S-matrix approach to the equation of state of dilute nuclear matter

J N DE*, S K SAMADDAR and B K AGRAWAL
Theory Division, Saha Institute of Nuclear Physics, 1/AF Bidhannagar, Kolkata 700 064, India
*Corresponding author. E-mail: jn.de@saha.ac.in

DOI: 10.1007/s12043-014-0711-z; ***e*Publication:** 1 April 2014

Abstract. Based on the general analysis of the grand canonical partition function in the S-matrix framework, a method is presented to calculate the equation of state of dilute warm nuclear matter. The result is a model-independent virial series for the pressure and density that systematically includes contributions from all the ground and excited states of all the stable nuclear species and their scattering channels. The multiplicity distribution of these species to keep the matter in statistical equilibrium is found out and then the pressure, incompressibility and the symmetry energy of the system are evaluated. The calculated symmetry energy coefficients are found to be in fair agreement with the recent experimental data.

Keywords. Symmetry energy; symmetry entropy; nuclear matter; statistical mechanics; S-matrix.

PACS Nos 12.40.Ee; 21.65.Mn; 21.65.Ef; 24.10.Pa

1. Introduction

The nuclear equation of state (EOS) plays the central role in our understanding of the properties of supernova dynamics or of neutron star matter in the cosmic context and of the physics of energetic heavy-ion collisions in the laboratory. Information on the EOS near the saturation density ρ_0 could be gleaned from empirical observations of certain macroscopic parameters defining the EOS (such as the energy per nucleon e [1], the isoscalar nuclear incompressibility K_∞ [2], the symmetry energy coefficient $e_{\rm sym}$ [1,3], or its density derivative L [4–6]). At higher density, the EOS is very uncertain and is model-dependent. At low densities, the system does not remain homogeneous, it minimizes free energy by forming clusters. One could deal with the EOS at these densities in sophisticated microscopic framework [7,8], but the shadow of model dependence could not be dispensed with.

A more direct approach for calculating the thermodynamic state functions based completely on observables was formulated long ago by Beth and Uhlenbeck [9] by expressing the said functions as a series expansion in density (the virial expansion). The second coefficient in the virial expansion for pressure of a low-density system (a gas) was expressed in terms of experimentally measurable two-body scattering phase shifts of its basic constituents (neutrons and protons, for nuclear matter and their bound states). But going beyond the second virial is proved very difficult [10], and so the theory cannot be fully trusted except for very dilute systems.

Recently, inclusion of bound states of more than two nucleons was attempted in the Beth–Uhlenbeck scheme for the calculation of nuclear EOS by Horowitz and Schwenk and coworkers [11,12]. They included the light nuclear species, namely neutron (n), proton (p), deuteron (d), triton (t), $He^3(h)$ and $He^4(\alpha)$, explicitly in the definition of the grand canonical partition function of the system and then calculated, in terms of their experimental binding energies and scattering phase shifts, the thermodynamic functions such as pressure or densities of the fragment species ρ_i that could remain in statistical equilibrium at a given temperature. Inclusion of a few more degrees of freedom other than n, p and d is seen to modify the nuclear EOS; as an example, the larger binding energy of the α-particle enhances its formation in the system and then lowers the pressure.

Noting that new degrees of freedom change the nuclear EOS, it is incumbent to consider the complete expression for the grand canonical partition function, as applied to nuclear matter, including all the heavier species and the scattering channels formed by them. We try to achieve this in the framework of the S-matrix formulation of statistical mechanics, as proposed by Dashen *et al* [13]. Starting from the elementary species (in nuclear matter, they are neutrons and protons) in the definition of the grand partition function, its calculation ends up with a multispecies system, with all the bound states treated on the same footing as the original elementary species. The complete formula involves two separate pieces. The first one is a sum of ideal gas terms, one for each of these species. The second piece originates from all possible scatterings of any number of particles from these species. This piece is in the form of a virial sum over all the scattering channels of terms involving their S-matrix elements. For light clusters, it involves their binding energies and their experimental scattering phase shifts. For the massive particles, the experimental phase shifts are not known, they are approximated by assuming resonance domination [14,15] of the S-matrix elements for scattering channels. It gives additional ideal gas terms from these resonances. As we would see, at very low densities or at high temperatures, the heavy clusters may not matter much, but at somewhat higher densities or at lower temperatures, they play a significant role in defining the thermodynamic variables such as pressure or entropy.

The paper is organized as follows. In §2, some details of the theory are given. Results and discussions are given in §3 and the concluding remarks are given in §4.

2. Elements of theory

Statistical mechanics in the S-matrix approach is the logical edifice on which our calculation is built. For two-component nuclear matter with the elementary species neutrons and protons, the grand canonical partition function is written as

$$\mathcal{Z} = \mathrm{Tr}\, \mathrm{e}^{-\beta(H-\mu_p\hat{N}_p-\mu_n\hat{N}_n)}\,, \tag{1}$$

where β is the inverse of temperature T of the system, H is the total Hamiltonian, $\hat{N}_{p,n}$ is the number operators for protons and neutrons, and $\mu_{p,n}$ are the corresponding chemical potentials. The trace is taken over any complete set of states of all possible number of nucleons. The full trace can be decomposed as

$$\mathcal{Z} = \sum_{Z,N=0}^{\infty} \zeta_p^Z \zeta_n^N \mathrm{Tr}_{Z,N}\, \mathrm{e}^{-\beta H}, \tag{2}$$

where the elementary fugacities are given by $\zeta_p = \mathrm{e}^{\beta\mu_p}$ and $\zeta_n = \mathrm{e}^{\beta\mu_n}$. The trace $\mathrm{Tr}_{Z,N}$ is taken over states of Z protons and N neutrons. For small ζ_p and ζ_n, the quantity $\ln\mathcal{Z}$ can be expanded in a virial series

$$\ln \mathcal{Z} = {\sum_{Z,N}}' D_{Z,N} \zeta_p^Z \zeta_n^N. \tag{3}$$

The prime on Σ indicates that the term with $Z = N = 0$ is excluded. The main task is to calculate the virial coefficients $D_{Z,N}$.

Following ref. [13], all the dynamical information concerning the microscopic interaction in the grand potential of the system can be collected in two types of terms, so that

$$\ln \mathcal{Z} = \ln \mathcal{Z}_{\text{part}}^{(0)} + \ln \mathcal{Z}_{\text{scat}} \tag{4}$$

corresponding to contributions from stable single-particle states of clusters of different sizes (neutrons and protons included) behaving like an ideal quantum gas and contributions coming from multiparticle scattering states. The particle piece can further be split into contributions from ground states and from particle-stable excited states, so that

$$\ln \mathcal{Z}_{\text{part}}^{(0)} = \ln \mathcal{Z}_{\text{gr}}^{(0)} + \ln \mathcal{Z}_{\text{ex}}^{(0)}. \tag{5}$$

The first term in eq. (5) is a sum of ideal gas terms, one for each of the ground states of all the species of mass number A with Z protons and N neutrons.

$$\ln \mathcal{Z}_{\text{gr}}^{(0)} = \mp V \sum_{Z,N} g_0 \int \frac{\mathrm{d}^3 p}{(2\pi)^3} \ln\left(1 \mp \zeta_{Z,N} \mathrm{e}^{-\beta(p^2/2Am)}\right). \tag{6}$$

In eq. (6), the $\mp$ sign corresponds to nuclei with A even or odd, obeying Bose or Fermi statistics, V is the volume of the system, g_0 is the spin degeneracy of the ground states of the nuclei, p is their momentum, m is the nucleon mass and $\zeta_{Z,N} = \mathrm{e}^{\beta(\mu_{Z,N}+B_{Z,N})}$ is the effective fugacity of the nuclear species. $B_{Z,N}$ is the binding energy of the nucleus and $\mu_{Z,N}$ is its chemical potential with $\mu_{Z,N} = Z\mu_p + N\mu_n$, reflecting chemical equilibrium among the different species in the system. Though Coulomb interaction is switched off in nuclear matter, we include its effect on the binding energies of nuclei, so that our calculation can be readily applied to a physical system such as supernova matter or neutron star matter, by including effects from the added electrons to make the system electrically neutral. Equation (6) can be readily expanded in a virial series as

$$\ln \mathcal{Z}_{\text{gr}}^{(0)} = V \sum_{Z,N} \frac{g_0}{\lambda_A^3} \left(\zeta_{Z,N} \pm \frac{\zeta_{Z,N}^2}{2^{5/2}} + \cdots\right), \tag{7}$$

provided $|\zeta_{Z,N}| < 1$. Here, $\lambda_A = \sqrt{2\pi/(AmT)}$ is the thermal wavelength of the species of mass number A. We work in natural units $\hbar = c = 1$. A nucleus in a particular excited (particle-stable) state can be taken as a distinctly different species and can be treated on the same footing as the ground state. The second term in eq. (5) takes care of the contributions from the excited states. In the same spirit of eq. (6), it can be written as

$$\ln \mathcal{Z}_{\text{ex}}^{(0)} = \mp V {\sum_{Z,N}}' \int_{E_0}^{E_{\text{s}}} \mathrm{d}E\, \omega(A,E) \times \int \frac{\mathrm{d}^3 p}{(2\pi)^3} \ln\left(1 \mp \zeta_{Z,N} \mathrm{e}^{-\beta(p^2/2Am+E)}\right), \tag{8}$$

where $\omega(A, E)$ is the level density of the excited states of a nucleus of mass A at an excitation energy E. For the level density, we take the expression [16]

$$\omega(A,E) = \frac{\sqrt{\pi}}{12a^{1/4}} \frac{\mathrm{e}^{2\sqrt{aE}}}{E^{5/4}}. \tag{9}$$

The level density parameter a is taken as $A/8$ MeV^{-1}, its empirical value. The prime on the sum in eq. (8) denotes exclusion of nuclei with $A \leq 8$. For these light nuclei, we consider only their ground states and their spin degeneracies are taken from experiments. For other nuclei, g_0 is taken to be 1 or 2 for the ground states depending on whether the nuclei are bosonic or fermionic. The lower limit E_0 in eq. (8) reflects the first excited state, the upper limit E_{s} is the nucleon separation energy. We take them to be 2 and 8 MeV, respectively, independent of the mass of the nuclear clusters. The scattering piece $\ln \mathcal{Z}_{\text{scat}}$ of eq. (4) in the context of nuclear matter can be written as [17]

$$\ln \mathcal{Z}_{\text{scat}} = V \sum_{Z_t,N_t} \frac{\mathrm{e}^{\beta\mu_{Z_t,N_t}}}{\lambda_{A_t}^3} \sum_{\sigma} \mathrm{e}^{\beta B_{Z_t,N_t,\sigma}} \times \int_0^\infty \mathrm{d}\epsilon\, \mathrm{e}^{-\beta\epsilon} \frac{1}{2\pi i} \mathrm{Tr}_{Z_t,N_t,\sigma} \left(\mathcal{A} S^{-1}(\epsilon) \frac{\partial}{\partial \epsilon} S(\epsilon)\right)_c. \tag{10}$$

In eq. (10), the double sum refers to the sum over all possible scattering channels, each having its chemical potential μ and formed by taking any number of particles from any of the stable species in their ground or excited states. The trace is over all plane-wave states for each of these channels. S is the scattering operator and $\mathcal{A}$ is the symmetrization or antisymmetrization operator (depending on whether the number of nucleons in the channels is even or odd) and the subscript c in parenthesis denotes that only the connected parts in the diagrammatics of the expression be taken into account. A channel in the set has a total number Z_t of protons and N_t of neutrons ($A_t = Z_t + N_t$); σ denotes all the other labels required to fix a channel and $B_{Z_t,N_t,\sigma}$ is the sum of the individual binding energies of all the particles in the channel and ϵ is the total kinetic energy in the centre of mass frame of the scattering partners. From eq. (10), it becomes clear that channels with larger binding energies are important because of the factor $\mathrm{e}^{\beta B_{Z_t,N_t,\sigma}}$, also two-particle channels dominate over multiparticle channels with the same Z_t and N_t from binding energy considerations. Only two-particle scattering channels are therefore considered. We further separate the channels into two parts, one consisting of low-mass particles

($A \leq 8$, say) and the other of heavy ones, containing at least one particle with mass $A > 8$. We thus write

$$\ln \mathcal{Z}_{\rm scat} = \ln \mathcal{Z}_{\rm L} + \ln \mathcal{Z}_{\rm H} \tag{11}$$

as the sum of contributions from the light (L) and heavy (H) channels.

The scattering of heavy nuclei is known to be dominated by a multitude of narrow resonances near the continuum threshold. The S-matrix elements are then approximated by the resonances. Each of these resonances can be treated as an ideal gas term [14,15]. Assuming the resonance level densities to be of the same form as that given in eq. (9), $\ln \mathcal{Z}^{\rm H}_{\rm scat}$ can then be written in the form of $\ln \mathcal{Z}^0_{\rm ex}$. The contributions from the excited and the resonance states can then be summed up and written as

$$\begin{aligned}\ln \mathcal{Z}^{(0)}_{\rm ex} + \ln \mathcal{Z}^{\rm H}_{\rm scat} &= \mp V {\sum_{Z,N}}' \int_{E_0}^{E_{\rm r}} {\rm d}E\ \omega(A,E) \\ &\quad \times \int \frac{{\rm d}^3 p}{(2\pi)^3} \ln\left(1 \mp \zeta_{Z,N} {\rm e}^{-\beta(p^2/2Am+E)}\right), \\ &= V {\sum_{Z,N}}' \frac{1}{\lambda_A^3}\left(f_1 \zeta_{Z,N} \pm f_2 \frac{\zeta^2_{Z,N}}{2^{5/2}} + \cdots\right).\end{aligned} \tag{12}$$

The integration in eq. (12) extends upto $E_{\rm r}$, the limit of resonance domination. The presence of the Boltzmann factor in the integral limits the contributions to only those from low energies. We take $E_{\rm r} = 12$ MeV. The functions f_n

$$f_n(A) = \int_{E_0}^{E_{\rm r}} {\rm d}E \omega(A,E) {\rm e}^{-n\beta E} \tag{13}$$

with $n = 1, 2, \ldots$ decreasing steadily with increasing n, and so the series converges quite fast.

For evaluating the contribution of the light particles $\ln \mathcal{Z}_{\rm L}$, only the scattering channels NN, Nt, $N{\rm He}^3$, $N\alpha$ and $\alpha\alpha$ are considered. Then

$$\ln \mathcal{Z}_{\rm L} = \ln \mathcal{Z}_{\rm NN} + \ln \mathcal{Z}_{Nt} + \ln \mathcal{Z}_{N{\rm He}^3} + \ln \mathcal{Z}_{N\alpha} + \ln \mathcal{Z}_{\alpha\alpha}. \tag{14}$$

Each of the terms in eq. (14) can be expanded in the respective virial coefficients. Expansion upto second order is only considered, the coefficients in second order are written as energy integrals in terms of relevant experimental phase shifts. As an example

$$\ln \mathcal{Z}_{NN} = V \frac{2}{\lambda_N^3}\left(\zeta_n + \zeta_p + \frac{b_{nn}}{2}\zeta_n^2 + \frac{b_{pp}}{2}\zeta_p^2 + \frac{1}{2} b_{np}\zeta_n\zeta_p\right) \tag{15}$$

with the virial coefficients,

$$b_{nn} = -\frac{1}{2^{3/2}} + \frac{\sqrt{2}}{\pi T}\int_0^\infty {\rm d}E \delta^{\rm tot}_{nn}(E){\rm e}^{-\beta E/2} \tag{16}$$

and

$$b_{np} = -6\sqrt{2} + \frac{\sqrt{2}}{\pi T}\int_0^\infty {\rm d}E \delta^{\rm tot}_{np}(E){\rm e}^{-\beta E/2} + 6\sqrt{2}{\rm e}^{B_d/T}. \tag{17}$$

In the limits of isospin symmetry, we take $b_{nn} = b_{pp}$. In eq. (17), the first two terms on the right-hand side (rhs) added together correspond to the non-resonant n–p scattering contribution; the last term is the resonant contribution coming from the bound state of the deuteron with binding energy B_d.

The total grand partition function for the interacting nuclear system is then given as

$$\ln \mathcal{Z} = \ln \mathcal{Z}^0_{\rm gr} + (\ln \mathcal{Z}^0_{\rm ex} + \ln \mathcal{Z}_{\rm H}) + \ln \mathcal{Z}_{\rm L}. \tag{18}$$

The relevant thermodynamic observables can then be calculated from the partition function [18,19]. For example, the pressure is evaluated from

$$P = T \ln \mathcal{Z}/V, \tag{19}$$

the number density ρ_i of the ith fragment species is calculated from

$$\rho_i = \zeta_i \left(\frac{\partial}{\partial \zeta_i} \frac{\ln \mathcal{Z}}{V} \right)_{V,T}, \tag{20}$$

or the entropy density $\mathcal{S}$ from

$$\mathcal{S} = \left(\frac{\partial P}{\partial T} \right)_{\mu}. \tag{21}$$

The free energy density $\mathcal{F}$ can be calculated from the Gibbs–Duhem relation, and the energy density $\mathcal{E}$ is evaluated once $\mathcal{S}$ is known.

3. Results and discussions

In calculating the nuclear EOS of dilute nuclear matter in the S-matrix approach, we have focussed on the pressure, nuclear incompressibility and the symmetry energy coefficient. The multiplicity distribution in the clusterized nuclear matter has also been computed. To make the results compatible with stellar dynamics, Coulomb term in the binding energies is taken into consideration. Without the Coulomb term, the number of fragment species in nuclear matter in principle becomes infinity, with its inclusion, the number becomes limited to ~ 8800 [20] with $A_{\rm max} = 339$ and $Z_{\rm max} = 136$. Experimental binding energies are taken as inputs when they are known. Otherwise those obtained from phenomenological studies [20] are used. The model with all these fragment species considered for calculations is termed as the inclusive species model (ISM). To understand the role of the heavy species on the thermodynamic observables, the S-matrix calculations have also been repeated with only the light species (n, p, d, t, ^{3}He and α). This truncated model is referred to as the light-species model (LSM).

In figure 1, the pressure as a function of density is displayed at two temperatures, T = 5 MeV (upper panel) and T = 10 MeV (lower panel), in LSM (red dashed lines) and also in ISM (blue full lines). Inclusion of heavier fragments lowers the pressure. For an ideal gas of fragments of different sizes, the pressure (contribution to pressure from scattering terms is comparatively smaller) is $\sim (N_k/V)T$, where N_k is the total number of fragments. When heavier species are included, N_k becomes smaller because of baryon

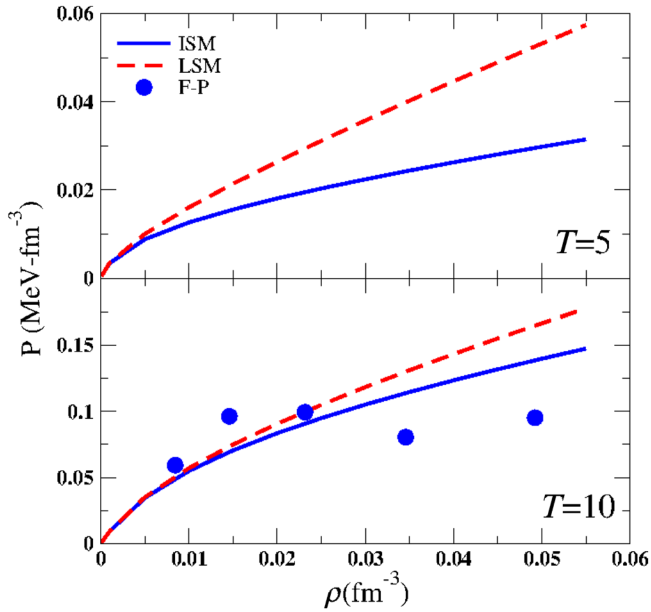

Figure 1. Plot of pressure vs. density at $T = 5$ and 10 MeV for symmetric nuclear matter. The red dashed lines represent calculations in LSM, the blue lines do so in ISM (see text for explanation of LSM and ISM). The blue filled circles are the microscopic results from ref. [7].

number conservation. At low temperature, with increased density, condensation of matter into heavy fragments becomes more favourable. The widening gap between the results from LSM and ISM at $T = 5$ MeV is an indication to this fact. Increasing temperature inhibits clusterization to heavier sizes. This is indicated in the lower panel of the figure where at the higher temperature $T = 10$ MeV, the pressure obtained from LSM and ISM are seen to come closer. Results from the microscopic calculation from ref. [7] at this temperature are also shown (as blue dots) for a comparison. The full many-body correlations responsible for clustering to heavier systems is absent in such a calculation; beyond a density $\rho \sim 0.05$ fm^{-3}, the system starts entering an unphysical region where incompressibility is negative. At $T = 5$ MeV, such a situation arises much earlier at lower density values.

The multiplicity distribution of the clusterized nuclear species at two densities ($\rho = 0.01$ and 0.02 fm^{-3}) and at two temperatures ($T = 5.0$ and 10.0 MeV) are presented in the four panels of figure 2. The blue full lines refer to calculations in ISM, the red dots do the same in LSM. The following conclusions can be drawn from an examination of the panels of this figure: (i) At low temperatures, in LSM (when $A_{\max}$ is 4), there is a preponderance of α-like clusters. When heavy species are included in the calculations, structure with a marked peak at α with non-negligible presence of some heavier nuclei is seen. The large binding energy of α favours its formation. (ii) When temperature is raised, the heavier fragments dissolve to lighter nuclei and there is not much difference in the multiplicities in the LSM and ISM. (iii) When density is higher, relatively higher

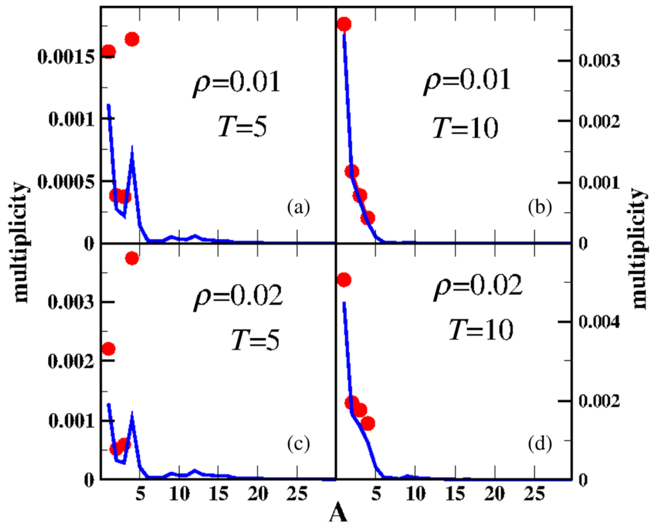

Figure 2. The fragment multiplicity distribution from symmetric nuclear matter shown as a function of the mass number A of the nuclear species at two densities and two temperatures as marked. The red dots are results from LSM, the blue lines refer to calculations in ISM.

percentage of α-particles are produced in LSM. In ISM, heavier species are also present; increasing temperature melts them to lighter species.

The density dependence of the compression modulus $K(=9(\mathrm{d}P/\mathrm{d}\rho))$ of dilute clusterized matter (calculated in ISM) is displayed in figure 3 at $T = 6$ and 10 MeV and is compared with that obtained from the mean-field (MF) model with a suitable effective nucleon–nucleon interaction (SKM* in the present case). Calculations at $T = 6$ MeV are presented as blue lines, those at $T = 10$ MeV by red lines. The full lines refer to results in the S-matrix formulation, the dashed lines are the ones from the MF model. At very very low density, both results agree with that expected for an ideal gas ($K = 9T$). As density increases, the MF and S-matrix results start deviating from each other.

In the MF model, in the density region we explore, the nuclear incompressibility decreases with density, ultimately becoming negative (the homogeneous nuclear system behaves like a Van der Waals fluid; with increasing density, in the MF model, the system enters the unphysical region, the point of entrance depending on temperature). The S-matrix approach also yields the compressibility modulus $K(\rho)$ that decreases with density, but it always remains positive in its region of applicability.

In inhomogeneous supernova matter, symmetry energy has a decisive role in neutrino-driven energy transfer [21] or in the explosive shock mechanism [22]. Defining symmetry energy or symmetry energy coefficients for clusterized nuclear matter, however, poses a problem [18,23]. Even symmetric nuclear matter, when warm and dilute, because of its composition of many asymmetric species, may have a sizeable symmetry energy content. For very low-density matter composed of only n, p, d and α, one does not face this problem though. Considering this composition, Horowitz and Schwenk [11] evaluated the symmetry energy coefficients of dilute nuclear matter and found them to be considerably

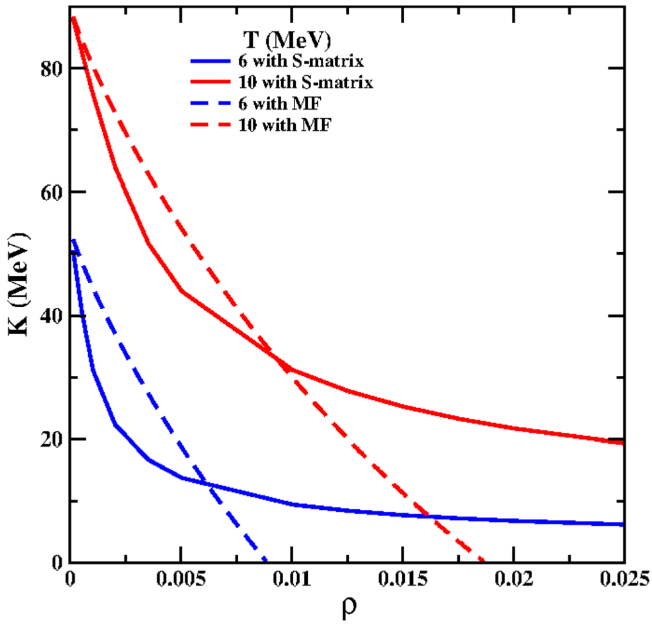

Figure 3. Incompressibility of symmetric nuclear matter shown as a function of density. The red lines correspond to $T = 10$ MeV, the blue lines to $T = 6$ MeV. The dashed lines are results from the mean-field model, the full lines are those from the S-matrix approach.

larger than those calculated in the MF prescription. Recently, there have been attempts [24,25] to measure the symmetry energy coefficients from heavy-ion collision experiments. The isoscaling technique [26] has been exploited to extract them, the temperature of the hot disassembled matter formed in collision is calculated from double-isotope ratio [27] and its density calculated from single-isotope ratio. In figure 4, we display the experimentally evaluated temperature, density and the symmetry energy coefficient $e_{\rm sym}$ from the recent experiment [25] and compare them with the theoretically calculated values. To avoid confusion, we define the symmetry energy coefficient as

$$e_{\rm sym} = e(\rho, \delta = 1, T) - e(\rho, \delta = 0, T), \tag{22}$$

a definition used by the experimentalists [25] in the context of constructing the symmetry coefficients from the experimental data. In eq. (22), e is the energy per nucleon and δ is the isospin asymmetry of the disassembled system. In the figure, the experimental points are shown as filled blue circles as a function of $v_{\rm surf}$ where $v_{\rm surf}$ is the velocity before the final Coulomb acceleration [24]; in essence, it is a measure of the temperature of the system. The theoretically calculated values are shown as filled red squares. The change in density or temperature at the same $v_{\rm surf}$ comes from the experimentally measured de-excited secondary fragments after correcting for particle emission and scattering effects [23,28,29]. These subtle changes call for a re-examination of the efficacy of isotope thermometry in the determination of temperature and density in heavy-ion collisions. Nevertheless, it is

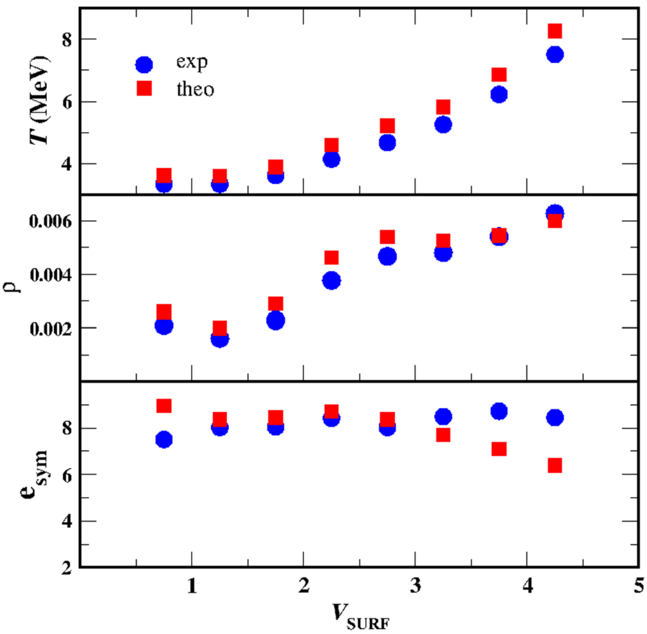

Figure 4. The extracted experimental values (blue circles) of temperature and density from ref. [25] are compared in the top and middle panels with the scattering-corrected values (red squares) obtained in the S-matrix framework in ISM. In the bottom panel, the experimental and theoretical values for the symmetry energy coefficient e_{sym} are presented for the corresponding temperature and densities, respectively.

seen that the calculated values of e_{sym} obtained from the definition given by eq. (22) agree very well with those obtained from experiments, except at very high temperatures.

4. Conclusions

Dilute warm matter cannot remain homogeneous, it disassembles into an inhomogeneous mixture of drops of unequal sizes to attain stability. In pursuing the statistical mechanics of such a system to find its composition in an S-matrix approach, we focussed on dilute nuclear matter and found out its equation of state with special emphasis on its pressure, incompressibility and the symmetry energy coefficient. The advantage of this approach is that all the observables can be directly connected to experimentally measured entities like the binding energy of clusters and the scattering phase shifts. No interaction potential enters the picture and so the results are mostly model independent.

In comparison to the MF model, the many-body correlations as embodied in the clustered structure of low-density nuclear matter reduces the pressure, increases the symmetry coefficients and also has a subtle effect on the nuclear incompressibility. These findings warrant a reckoning as they have immediate applicability in supernova simulation dynamics. No direct experimental measurement of pressure or incompressibility of dilute nuclear matter has yet been made or suggested. Of late, symmetry energy of such systems has been measured; they seem to be in good consonance with those obtained from our theoretical calculations. A cautionary note is, however, in order. The definition of symmetry energy for clusterized matter suffers from ambiguity [23] and therefore except for very very dilute systems, a model dependence in the experimental extraction or in their theoretical comparison cannot be avoided.

Acknowledgements

JND and SKS acknowledge the support from the Department of Science & Technology, Government of India.

References

[1] P Möller *et al*, *Phys. Rev. Lett*. **108**, 052501 (2012)
[2] J P Blaizot, *Phys. Rep.* **64**, 171 (1980)
[3] H Jiang, G J Fu, Y M Zhao and A Arima, *Phys. Rev. C* **85**, 024301 (2012)
[4] M Centelles, X Roca-Maza, X Viñas and M Warda, *Phys. Rev. Lett.* **102**, 122502 (2009)
[5] B K Agrawal, J N De and S K Samaddar, *Phys. Rev. Lett.* **109**, 262501 (2012)
[6] B K Agrawal, J N De, S K Samaddar, G Colò and A Sulaksono, *Phys. Rev. C* **87**, 151306(R) (2013)
[7] B Friedman and V R Pandharipande, *Nucl. Phys. A* **361**, 502 (1981)
[8] A Akmal, V R Pandharipande and D G Ravenhall, *Phys. Rev. C* **58**, 1804 (1998)
[9] E Beth and G E Uhlenbeck, *Physica* **4**, 915 (1937)
[10] A Pais and G E Uhlenbeck, *Phys. Rev.* **116**, 250 (1959)
[11] C J Horowitz and A Schwenk, *Nucl. Phys. A* **776**, 55 (2006); *Phys. Lett. B* **638**, 153 (2006)
[12] E O'Connor, D Gazit, C J Horowitz, A Schwenk and M Barnea, *Phys. Rev. C* **75**, 055803 (2007)
[13] R Dashen, S-K Ma and H J Bernstein, *Phys. Rev.* **187**, 345 (1969)
[14] R Dashen and R Rajaraman, *Phys. Rev. D* **10**, 694 (1974)
[15] R Dashen and R Rajaraman, *Phys. Rev. D* **10**, 708 (1974)
[16] A Bohr and B R Mottelson, *Nuclear structure* (W.A. Benjamin Inc., 1969) Vol. I
[17] S Mallik, J N De, S K Samaddar and Sourav Sarkar, *Phys. Rev. C* **77**, 032201(R) (2008)
[18] J N De and S K Samaddar, *Phys. Rev. C* **78**, 065204 (2008)
[19] S K Samaddar, J N De, X Viñas and M Centelles, *Phys. Rev. C* **80**, 035803 (2009)
[20] W D Myers and W J Swiatecki, *Nucl Phys. A* **601**, 141 (2003) (Lawrence Berkeley Laboratory Report, LBL-36803)
[21] H-Th. Janka *et al*, *Phys. Rep.* **442**, 38 (2007)
[22] A W Steiner, M Prakash, J M Lattimer and P J Ellis, *Phys. Rep.* **411**, 325 (2005)
[23] J N De, S K Samaddar and B K Agrawal, *Phys. Rev. C* **82**, 045201 (2010)
[24] S Kowalski *et al*, *Phys. Rev.C* **75**, 014601 (2007)
[25] J B Natowitz *et al*, *Phys. Rev. Lett.* **104**, 202501 (2010)
[26] A Ono *et al*, *Phys. Rev. C* **68**, 051601(R) (2003)
[27] S Albergo, S Costa, E Costanzo and A Rubbino, *Nuovo Cimento A* **89**, 1 (1985)
[28] S K Samaddar and J N De, *Phys. Rev. C* **79**, 051602(R) (2009)
[29] S K Samaddar and J N De, *Phys. Rev. C* **81**, 041601(R) (2010)